# Contactless Finger Tapping Detection at C Band

Xiaodong Yang, Lei Guan, Yajun Li, Weigang Wang, Qing Zhang, Masood Ur Rehman and Qammer Hussain Abbasi

***Abstract*—The rapid finger tap test is widely used in clinical assessment of dyskinesias in Parkinson's disease. In clinical practice, doctors rely on their clinical experience and use the Parkinson's Disease Uniform Rating Scale to make a brief judgment of symptoms. We propose a novel C-band microwave sensing method to evaluate finger tapping quantitatively and qualitatively in a non-contact way based on wireless channel information (WCI). The phase difference between adjacent antennas is used to calibrate the original random phase. Outlier filtering and smoothing filtering are used to process WCI waveforms. Based on the resulting signal, we define and extract a set of features related to the features described in UPDRS. Finally, the features are input into a support vector machine (SVM) to obtain results for patients with different severity. The results show that the proposed system can achieve an average accuracy of 99%. Compared with the amplitude, the average quantization accuracy of the phase difference on finger tapping is improved by 3%. In the future, the proposed system could assist doctors to quantify the movement disorders of patients, and it is very promising to be a candidate for clinical practice.**

***Index Terms*—finger taps, non-contact, phase difference, SVM, UPDRS, WCI**

## I. INTRODUCTION

Quantification of human dyskinesia has been a one of the prominent smart health research area in recent years. Take Parkinson as an example, Medical manifestations mainly include motor symptoms and non-motor symptoms. Among them [1] the main symptoms of exercise are static tremor, myotonic, bradykinesia and posture balance disorder. Non-motor symptoms are mainly sleep disorders, autonomic dysfunction, and mental disorders [2]. Dyskinesia is the main cause of disability in Parkinson's patients. It not only affects the life of patients but also increases the liability of care takers.

In order to identify Parkinson's patients and accurately assess their motor function, the researchers have been trying various means to quantify dyskinesia in patients with Parkinson's disease, including frozen gait [3-4], repetitive eye-hand movement [5] and finger tapping. Especially for the evaluation of Parkinson's disease (PD), finger tapping is widely used in clinical practice. The reasons are as follows: the rhythm of finger movement is an effective index to evaluate the function of brain movement [6]. Measuring the ability of individuals to fingers tap is an important method to evaluate the integrity of neuromuscular. In addition, there is a strong correlation between dopamine receptor and motor task of finger tapping in Parkinson's disease, the rhythm, amplitude and speed of the finger tapping movement vary with the patient's motor ability and symptoms.

In recent decades, the medical community has been developing clinical tools, such as rating scales to quantify the severity of motor and other symptoms of Parkinson's disease. UPDRS is still the preferred method because it is currently the most mature dyskinesia rating scale and easy to manage [6]. While observing several patients' motions such as upper-limb motion, walking, and "finger-tapping" motions, a doctor evaluates the degree of motor deterioration according to UPDRS. However, there are still some problems in clinical application: First, the assessment of dyskinesia mainly relies on the doctor's clinical experience and subjective judgment, which leads to the quantitative results not being completely objective. Second, the patient needs to go to the hospital for a diagnosis. When performing the test in the UPDRS motor part (III), the patient did not show any symptoms, which may lead to an inaccurate assessment.

Finger taps (patient taps thumb with index finger in rapid succession) severity is an indicator of quantifying Parkinson's. The severity of finger taps is divided into a total of 5 ratings ranges from 0 to 4 according to the UPDRS.

0: Normal.

1: Mild slowing and/or reduction in amplitude.

2: Moderately impaired. Definite and early fatiguing. May have occasional arrests in movement.

3: Severely impaired. Frequent hesitation in initiating movements or arrests in ongoing movement.

4: Can barely perform the task.

Many researchers are currently working on finding effective ways to quantify finger taps. The existing study on quantifying the severity of finger taps is mainly divided into two categories: one based on Micro-Electro-Mechanical System (MEMS) and the other based on computer vision. The advantages of MEMS, such as small size, low power consumption, low cost and wide range of uses, make it a tool for a large number of researchers and used to evaluate patients' movement disorders. These

Xiaodong Yang is with the School of Electronic Engineering, Xidian University, Xi'an 710071, China. (e-mail: xdyang@xidian.edu.cn)

Lei Guan is with the School of Life Science and Technology, Xidian University, Xi'an 710071, China.

Yajun Li, Weigang Wang, Qing Zhang are with the Northwest Women's and Children's Hospital, Xi'an Jiaotong University Health Science Center, Xi'an, Shaanxi, 710061, China.

Masood Ur Rehman and Qammer Hussain Abbasi are with the School of Engineering, University of Glasgow, Glasgow G12 8QQ, UK.

devices need to be worn on the patient. Gyro wearable systems are widely used to evaluate finger fitting tasks [ 7, 8,9 ,10]. The gyroscope is worn on the index finger of the subject [8,9] or wear on the index finger and thumb [9]. The severity of finger taps is quantified by evaluating speed, finger movement amplitude and motion rhythm. The tapping amplitudes can be quantified through angle excursions [11,12]. Acceleration sensors are also used to quantify the degree of damage to the finger [13,14 ,15,16]. Yokoe. M et al. [17] finds the opening and closing speed is the best parameter. These studies extract time domain features such as finger taps frequency [18], pause duration, number of halts and so on [19]. In addition, Yuko Sano et al. [20] proposed a system for measuring the severity of finger taps based on magnetic force. The subject's thumb and forefinger were attached to a magnetometer. The system outputs parameters such as distance, speed, acceleration and interval of finger movement during the finger taps task.

Taha Khan et al. [21] used a video camera to record the patient's finger taps video. They use computer vision algorithms to track moving fingers. Extracting different features from the time series estimates finger taps speed, amplitude, and rhythm. Stefan et al. [22] used DeepLabCut to track frame by frame video recordings of finger tapping on standard smartphones. They tracked hand localization points (including fingertips and thumb tips) by evaluating network capabilities, and extracted amplitude, distance, and rhythm to quantify finger tapping. Pang et al. [23] used discrete wavelet transform (DWT) to extract the (3D) motion features of each finger joint. The severity of each finger joint tremor was quantified by analyzing the frequency of motion changes. However, the user must maintain a line of sight with the camera. It must be mentioned that using camera detection will involve personal privacy.

Wireless sensing technology using channel observation has attracted the attention of researchers in recent years. The researchers found that wireless signals can sense and recognize changes in the environment. A lot of research work is done based on the amplitude of wireless channel information such as presence detection [24], indoor positioning [25 26], and crowd counting [27 28]. In addition, WCI is also widely used in human activity recognition applications [29,30,31,32]. It has been proven that it can be used for small-scale motion detection such as respiratory rhythm monitoring [33], lip recognition [34] and keystroke [35]. WCI phase shift is related to signal transmission delay and direction in space and frequency domain, which can be used for human localization and tracking [36]. The phase difference between adjacent antennas in time domain has different dominant frequency components, which can be used to estimate respiratory frequency [37].

Compared with previous work, the main purpose of this paper is to design a non-contact perception method to evaluate patients with movement disorders. The patient collects and evaluates the patient's motion signals without wearing any wearable devices. In addition, the wireless sensing method can effectively prevent leakage of user privacy. Our system uses a pair of simple wireless transceivers. The wireless signal transmitter continuously transmits wireless signals. During wireless signal propagation, the finger of the patient performing the finger taps task is considered an obstacle to the movement, so this factor causes disturbances in wireless signals, multipath propagation effects, reflections and delays. The receiver receives the wireless signal and extracts the constantly changing WCI. This provides a guarantee for continuous monitoring of the patient's hand movements. The WCI carrying amplitude and phase is obtained from the wireless signal. The original phase is calibrated by the phase difference between adjacent antennas. We use outlier detection and smooth methods to obtain a pure finger taps signal. Finally, the extracted features are input to the classifier to complete the evaluation of finger tapping.

In summary, the main contributions in this paper are as follows:

1. We propose a non-contact method to quantify the severity of finger taps. We use the WCI from the physical layer to detect the wireless signal interfered by finger. As far as we know, this is the first work to quantify the severity of finger taps using wireless signals.

2. Differences with other wireless sensing operations, we use the phase difference of adjacent antennas to process the wireless signals affected by finger taps. After data processing and feature extraction are performed, and then machine learning algorithm is used to classify the finger taps signals of different severity.

3. We performed experiments and verified the performance of our proposed system, with a classification accuracy of more than 98% for finger signals with different severity. Non-contact intelligent health monitoring is of great significance for the early treatment and detection of diseases.

The remainder of the article is organized as follow. Section II gives the basic theory of the wireless sensing technology leveraging WCI; Section III describe the system architecture; Section IV describes the experiment setup and discuss the experimental results. Finally, Section V concludes the article. In the following Table I, we summarize all the used abbreviations in this work to assist the reader.

TABLE I
LIST OF USED ABBREVIATIONS WITH THE DEFINITION

| Abbreviations | Definition |
|---|---|
| WCI | Wireless Channel Information |
| UPDRS | Unified Parkinson Disease Rating Scale |
| MEMS | Micro-Electro-Mechanical System |
| OFDM | Orthogonal Frequency Division Multiplexing |
| SVM | Support Vector Machine |
| CFR | Channel Frequency Response |
| DC | Direct Current |
| DWT | Discrete Wavelet Transform |

## II. FUNDAMENTAL

The proposed method is to analyze the wireless signal from the transmitting end and the receiving end in C band. The WCI is extracted by applying orthogonal frequency division multiplexing (OFDM) technique. WCI characterize by

multipath effects, reflections, scattering, shadowing and refraction. In OFDM data is divided into multiple orthogonal sub-carriers so that all sub-carriers can finely describe the WCI in each propagation path. We obtain the channel frequency response from the WCI of each sub-carrier.

In our sensing system, the channel frequency response (CFR) of 30 sub-carriers can be obtained in each received data packet. The CFR of these 30 subcarriers is expressed as follows:

$$\mathrm{H}(f) = [\mathrm{H}(f_1), \mathrm{H}(f_2), \ldots \mathrm{H}(f_n)] \quad (1)$$

The CFR of each sub-carrier containing amplitude and phase information is expressed as follows:

$$\mathrm{H}(f_s) = \|\mathrm{H}(f_s)\| exp\big(j\angle \mathrm{H}(f_s)\big) \quad (2)$$

where $f_s$ is the center frequency of the $s^{th}$ sub-carrier. $\|\mathrm{H}(f_k)\|$ is the amplitude of the $k$th subcarrier, $\angle \mathrm{H}(f_s)$ is the phase of the $s^{th}$ sub-carrier. The original amplitude and phase information is shown in Fig. 1. In order to continuously monitor the finger taps, the WCI is continuously recorded in the time window of length $D$ and it is expressed as:

$$\mathrm{H}_{total} = [\mathrm{H}_1, \mathrm{H}_2 \ldots \mathrm{H}_D\ ] \quad (3)$$

where total is the number of packets received. These $D$ wireless data contain the original information of the finger taps.

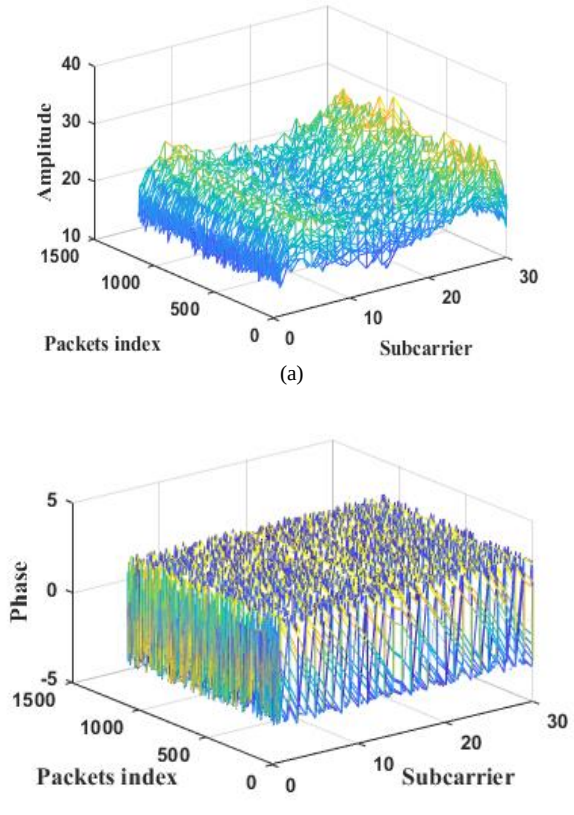


(a)

(b)

Fig. 1. (a)The row amplitude information of wireless channel information. (b) The row phase information of wireless channel information.

## III. SYSTEM DESIGN

In this section, we first introduce the structure of wireless signal-based sensing system. The system robustly quantifies the severity of finger taps. We then introduce methods of data processing and extraction of features.

### A. System architecture

Our wireless sensing system architecture is presented in Fig. 2. It consists of three main modules: (i) data extraction, (ii) data processing and (iii) classification. In the data extraction module, the transmitter sends a 5.32GHz wireless signal, and the receiver captures the wireless signal interfered by the finger. In the data processing module, we first calibrate the original phase using the phase difference of the adjacent antennas to obtain the WCI of the finger taps then removes outliers. Finally, we use local weighted regression algorithm to filter and smooth the finger tapping signal.

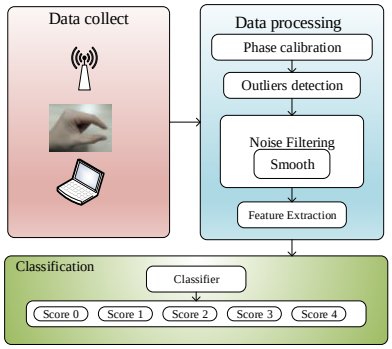


Fig. 2. System architecture.

### B. Phase calibration

The phase of the raw data exhibits a random distribution that cannot be used to identify motion and perceive environmental changes. Therefore, the phase information is not getting enough attention. In previous research work amplitude information of the WCI was considered for such applications while neglecting the phase information. In this paper, we use the phase difference between two adjacent antennas to calibrate the phase information. The purpose of this paper is to prove from the perspective of experimental results that phase difference data is better than amplitude information in quantifying finger taps. The uncalibrated phase of the $j^{th}$ subcarrier can be represented as:

$$\hat{\psi}_j = \psi_j - 2\pi \frac{k_j}{N} \delta + \beta. \quad (4)$$

where $\hat{\psi}_j$ denotes the true phase of CSI data, $\delta$ is offset timing, $\beta$ is the initial phase offset due to the phase-locked loop (PLL). $k_j$ indicates the sub-carrier number of the $j^{th}$ subcarrier and the $N$ is the FFT size which is equal to 64 in the IEEE 802.11a/g/n in wireless standard. In summary, it is difficult to obtain the available phase information from the wireless device.

The phase difference from adjacent antennas is stable and can be used to assess finger tap, because different antennas use the same system clock in the same wireless device. Therefore, the

phase difference information of adjacent antennas can be obtained by using the following equation:

$$\Delta\hat{\psi}_j = \Delta\psi_j - 2\pi\frac{k_j}{N}\Delta\delta + \Delta\beta. \quad (5)$$

where $\Delta\psi_j = \psi_{j1} - \psi_{j2}$, is the difference of true phase, $\Delta\delta = \delta_1 - \delta_2$ is the delay of each adjacent antenna, $\Delta\beta$ is the unknown difference in phase offsets, which is actually a constant [38]. For $\Delta\delta$, it can be expressed as follows:

$$\Delta\delta = \frac{d\sin\theta}{cT} \leq \frac{1}{2fT}. \quad (6)$$

where d is the distance between the antennas, $\theta$ is the direction of arrival, $c$ is the speed of light, T is the 50 ns Wi-Fi sampling interval and f is the frequency. Therefore, $\delta$ approaches 0 and $2\pi\frac{k_j}{N}\Delta\delta$ is ignored in $\Delta\hat{\psi}_j$. Therefore, the phase $\Delta\psi_j$ calibrated by the phase difference can be expressed as:

$$\Delta\hat{\psi}_j = \Delta\psi_j + \Delta\beta. \quad (7)$$

We find that the phase information after the phase difference processing became perfect, and the finger taps task could be finely depicted. However, the calibrated phase information has a DC component. We need to remove the DC component because the DC component affects the extraction of features such as peak detection and Fast Fourier frequency (FFT) detection. Specifically, the mean value of the phase difference signal is first calculated.

$$\bar{x} = \frac{1}{N}\sum_{i=1}^{N} x_i \quad (8)$$

where $\bar{x}$ is the DC component of the phase difference and $x_i$ is the phase difference information of the $i^{th}$ packet. Then, the calibration signal $\hat{x}_i$ is obtained by subtracting DC component from original phase information:

$$\hat{x}_i = x_i - \bar{x} \quad (10)$$

In order to show the difference between the phase being calibrated and the original phase in the finger taps experiment result is taken. In Fig. 3, the phase marked by red dots is the phase difference of adjacent antennas and the phase of the single antenna is marked by blue. We find that the phase of the single antenna without any processing is randomly distributed in [-π, π], which causes the original phase to be unusable. The phase of finger-tapping after phase difference processing is distributed in $[-\frac{\pi}{6}, \frac{\pi}{12}]$.

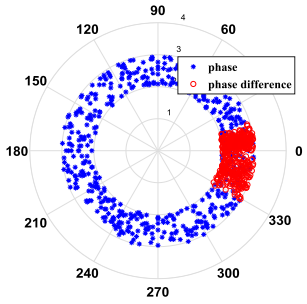


Fig. 3. Comparison between the phase (marked by blue) of a single antenna and the phase difference (marked by red) of two adjacent antennas.

Fig. 4(a) shows the finger tapping waveform of 30 carriers. Fig.4(b) shows the standard deviation of the finger tap waveforms of all subcarriers in this experiment, of which the 13th subcarrier has the largest variance. When there is a moving object in the transceiver device, the wireless signal will fluctuate. In other words, compared with other sub-carriers, the sub-carrier with the largest standard deviation is easier to obtain the finger tap signal. Therefore, we choose the sub-carrier with the largest variance to characterize finger tapping in this study.

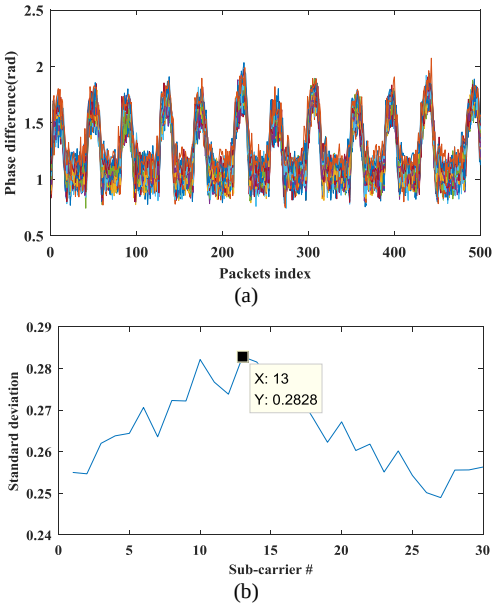


Fig. 4. (a) All subcarrier finger tapping waveforms. (b) Standard deviation of the subcarriers

## C. *Filter processing*

Due to the influence of environmental noise, protocol specifications and hardware, there are some abnormal phenomena, which are obviously not caused by human motion and affect the continuity of the signal. Therefore, it should be screened before human detection. We use the Hampel filter to detect the outliers which falling out of the closed interval $[m_i - \gamma * MAD_i, m_i + \gamma * MAD_i]$, where

$$m_i = median(x_i, x_{i+1} \dots x_{i+d}) \quad (10)$$
$$MAD_i = median(|x_i - m_i|, |x_{i+1} - m_i|, \dots |x_{i+k} - m_i|) \quad (11)$$

$d$ is the length of the sliding data window, $m_i$ is the median and $MAD_i$ is known as the median absolute deviation of the data sequence, $\gamma$ is the factor of violation and mostly used value is 3 [39]. Fig. 4 shows the phase difference of the sub-carrier before and after using removing outliers. The yellow waveform is the phase difference signal from which the abnormal point has been removed, and the blue waveform is the original phase difference signal. The marked points are outlier. We can see that the outliers are effectively filtered out and replaced by median value.

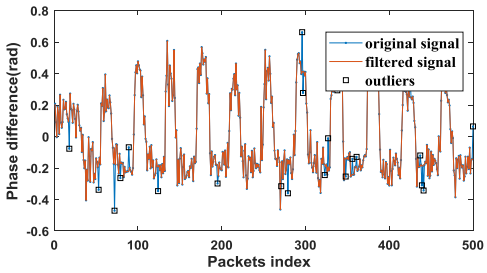


Fig. 5. Outlier removal on phase difference.

Although some obvious outliers have been removed, the waveform of finger tapping still has high-frequency noise. Due to the presence of noise, it is difficult to extract a series of features such as peaks and peak-to-peak values for continuous and periodic signal waveforms. Therefore, this study uses the local weighted regression algorithm to smooth the finger tapping waveform to achieve the filtering effect. The smoothing process is considered local because like the moving average method. Each smoothed value is determined by neighboring data points defined within the span [40]. The process is weighted because a regression weight function is defined for the data points contained within the span.

Step 1: the range of the points to be included is determined. The number $n$ of these points is specified. The larger this value is, the smoother the adapted curve will be in the end. The range is determined in such a way that exactly $n$ values, including the selected point itself, are in the range, and the selected point is in the center of the selected range.

Step 2: Establish weights for local weighted regression smoothing. The weights are given by the tricube function:

$$w_i = (1 - \left|\frac{x_0 - x_i}{\Delta(x_0)}\right|^3)^3 \tag{12}$$

$$\Delta(x_0) = \max_{x_i \in N} |x_0 - x_i| \tag{13}$$

Step 3: Perform regression smoothing. The LOESS procedure uses a quadratic function.

$$\hat{y}_k = a + bx_k + cx_k{}^2 \tag{14}$$

Step 4: For the finger tap signal, the data collected in each experiment is relatively small. In this case, the estimated regression function may be more or less strongly affected by potential outliers. We need to determine the robust weights. Therefore, robust weightings are determined in a fourth step of the procedure. To determine the weightings, the residuals of the values estimated up to this point and the resulting median are calculated. The calculation formula is as follows:

$$G(x_k) = \begin{cases} (1 - (\frac{|y_i - \hat{y}_i|}{6median(|y_i - \hat{y}_i|)})^2)^2, & \left|\frac{|y_i - \hat{y}_i|}{6median(|y_i - \hat{y}_i|)}\right| < 1 \\ 0 \quad , & \left|\frac{|y_i - \hat{y}_i|}{6median(|y_i - \hat{y}_i|)}\right| \geq 1 \end{cases} \tag{15}$$

If the residual is greater than or equal to 6 times the median, the robust weighting is 0. This achieves the purpose of smoothing. The robust weightings, multiplied with the proximity weightings, are used for re-estimating a linear regression function within the individual ranges:

$$\sum_k w(x_k)\, G(x_k)(y_k - a - bx_k - cx_k{}^2)^2 \tag{16}$$

A series of new smoothed values is the result.

The smoothed value is given by the weighted regression at the predictor value of interest. Fig. 6 illustrates the phase difference of a sub-carrier after using the smoothing filter. We can see that the smoothed signal become smoother after wavelet decomposition and provides accessibility for the extraction of some features.

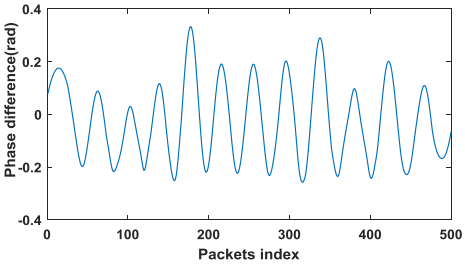


Fig. 6. Phase difference after smoothing filtering.

### *D. Feature extraction*

In order to accurately recognize the severity of finger taps, we define and extract features related to severity of finger taps according to the UPDRS. We detect the peaks and troughs of the phase difference waveform. Although the waveform become smoothed after smoothing but fake peaks still appear at the peak detection. We apply a threshold to the minimum distance between two adjacent peaks to eliminate the fake peak. i.e. the detected peak is regarded as the center of the data window. If the data in the data window is smaller than the peak value, the peak value is judged as a true peak, otherwise it is determined as a fake peak and removed. Then, we define the difference between adjacent peaks and troughs as the amplitude. To indicate the speed or frequency of the finger taps, we record the number of waveform peaks in the finger taps task. In addition, the phase difference signal is subjected to FFT. The frequency value corresponding to the maximum value in the FFT spectrum is recorded, and this value is considered as the frequency of finger taps. In addition to this, statistical time domain parameters are taken into account as features of finger tapping. All of the seven time domain parameters extracted are capable of emphasizing useful information in the signal. Root mean square helps track the total power of the signal. The waveform factor is the ratio of the DC signal information and the AC signal information of the signal. Skewness is used to

measure the degree of asymmetry of the signal. The standard deviation is the degree of dispersion of the signal. The kurtosis value is a measure of the tail of the probability distribution of a real-valued random variable. The crest factor characterizes the apparent extent of this signal peak. These features are the most intuitive and computationally simple statistical features of the signals that can be observed in the time domain. We list all the extracted feature columns and their corresponding expressions in the table II.

TABLE II
STATISTICAL TIME DOMAIN FEATURES OF FINGER TAPPING

| Feature | Feature definition |
|---|---|
| Total number of taps | N |
| Finger taps frequency | F |
| Amplitude | Peaks- troughs |
| Root mean square (RMS) | $\sqrt{\frac{1}{N}\sum_{i=1}^{N} x_i}$ |
| Wave form factor | $\frac{RMS}{\frac{1}{N}\sum_{i=1}^{N}\lvert x_i\rvert}$ |
| Impact factor | $\frac{\max(\lvert x_i\rvert)}{\frac{1}{N}\sum_{i=1}^{N}\lvert x_i\rvert}$ |
| Skewness value | $\frac{1}{N}\sum_{i=1}^{N}(\frac{x_i-u_x}{\sigma})^3$ |
| Standard deviation | $\sqrt{\frac{1}{N}\sum_{i=1}^{N}(x_i-u_x)^2}$ |
| Kurtosis value | $\frac{1}{N}\sum_{i=1}^{N}(\frac{x_i-u_x}{\sigma})^4$ |
| Crest factor | $\frac{\max(\lvert x_i\rvert)}{RMS}$ |

### *F. Classification Algorithms*

We use the SVM to quantify finger grips of different severity according to the UPDRS. As the mainstream technology of machine learning, SVM has shown excellent performance in classifying two classification and multi-classification tasks. SVM can be used in data analysis, pattern recognition, text classification and other fields. In a linearly separable data set, the goal of the SVM is to find a separate hyperplane that can accurately classify two types of data. In the multi-classification problem of finger taps with different severity, the following optimization problems are solved：

$$\min_{w,b,} \min \frac{1}{2}\|w\|^2 \tag{15}$$

$$\text{s.t. } y_i(w^T\phi(x_i+b)) \geqq 1, \quad i=1,2,\dots,m \tag{16}$$

where w is the weighting factor and b is the classification threshold, usually used for converting the (15) to the dual problem:

$$\max_{\alpha} \sum_{i=1}^{m}\alpha_i - \frac{1}{2}\sum_{i=1}^{m}\sum_{j=1}^{m}\alpha_i\alpha_j y_i y_j \kappa(x_i,x_j) \tag{17}$$

$$s.t. \sum_{i=1}^{m}\alpha_i y_i = 0, \alpha_i \geq 0, i=1,2,\dots,m. \tag{18}$$

where $\kappa(x_i,x_j)$ is the kernel function. SVM avoids the problem of dimensionality disaster by introducing a kernel function. This maps linearly inseparable samples to a higher-dimensional feature space, so that samples can be linearly separable in this high-dimensional space. In the case of a small number of samples, there is a significant advantage over other machine learning algorithms (MLA).

## IV. EXPERIMENTAL DESIGN

In this section, the experimental setup and implementation are described.

We did plenty of finger taps experiments in the lab environment. During the experiment, two Lenovo computers with ubuntu operating system were used as transmitter and receiver. We configure the wireless network card of the transmitter to the injection mode, and the wireless network card of the receiver to the monitoring mode. The transmitter is equipped with 1 omnidirectional antenna, the receiver is equipped with 2 omnidirectional antennas and the distance between the antennas is 5cm. The center frequency of the transmitted wireless signal is 5.32GHz, the transmission power is 15dBm, and the bandwidth is 20Mhz. The sampling frequency of the receiver is 50Hz, i.e. receiving 50 packets per second. The entire system forms a 1x2 single input multiple output (SIMO) system. The distance between the transmitting antenna and receiving antennas is 1m. In order to effectively detect the participant's finger tapping motion and reduce external interference, we use absorbing materials to surround the experimental scene. During the experiment, the participants placed their arms between the transceiver antenna and performed a finger tapping test. The experimental scene is shown in Fig7.

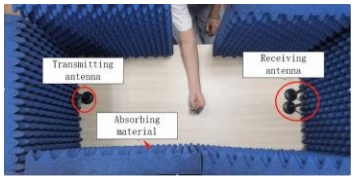

Fig. 7 Experimental scene

In this study, five volunteers were recruited. Before the experiment, each person read the finger tapping task item in the UPDRS form and watch the Parkinson patient finger taps task video. Learn and master the characteristics of the different severity of finger taps. In addition, during the volunteer training phase, each volunteer wore a three-axis acceleration sensor on his finger. We trained the volunteers according to the triaxial acceleration waveform of Parkinson's finger tapping in [19] and the characteristics described in UPDRS. The main characteristics of imitation include breaking the regular rhythm, interruption, and amplitude reduction. Figure 8 shows the normalized waveform that imitate the patient's finger tapping. Each person simulated different severity of finger taps tasks as required, and each level was simulated 10 times. During the

experiment, the subject placed the hand performing the finger taps task between the receiver and the transmitter, each experiment lasted for 10s and the interval between two adjacent tests was greater than 10s for the subject to rest.

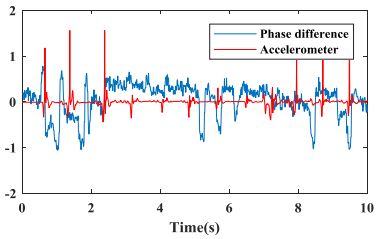


Fig. 8 The waveform of imitate the patient's finger tapping

## V. RESULTS AND DISCUSSION

The power of WCI measures the combination of all paths. The frequency, amplitude, speed and other characteristics of finger taps of different severity are different. Therefore, the speed of change of WCI reflected by finger movement is also different. We can use time-frequency analysis tools (such as short-time Fourier transform and discrete wavelet transform [26]) to separate the frequency components of the patient's hand motion to help us analyze the characteristics of finger tapping. For example, the DWT spectrograms corresponding to the participants of five different severity levels shown in Fig.7. The spectrogram shows how the energy of each frequency component evolves over time. The high energy component is displayed in red, and the low energy component is displayed in blue. As shown in Fig. 7(a)(f)(k)(p)(u), there is a high-energy band around 4~5hz in the spectrum chart of normal human finger tapping, which coincides with the normal finger tapping speed. Participants with severity level 1 have lower finger tapping speeds than normal people. The frequency of finger tapping is concentrated at 2~3 Hz as shown in Figure 7(b)(g)(l)(q)(v). The frequency of finger tapping of participants with severity level 2 concentrated at 1-2 Hz, as shown in Figure 7 (c) (h) (m) (r) (w).The frequency of finger tapping of participants with severity level 3 is distributed around 1 Hz as shown in Figure 7(d)(i)(n)(s)(x). Because participants with a severity level of 4 cannot complete this clinical task, the frequency spectrum is messy and the energy is concentrated around 0 Hz as shown in Figure 7(e)(j)(o)(t)(y).

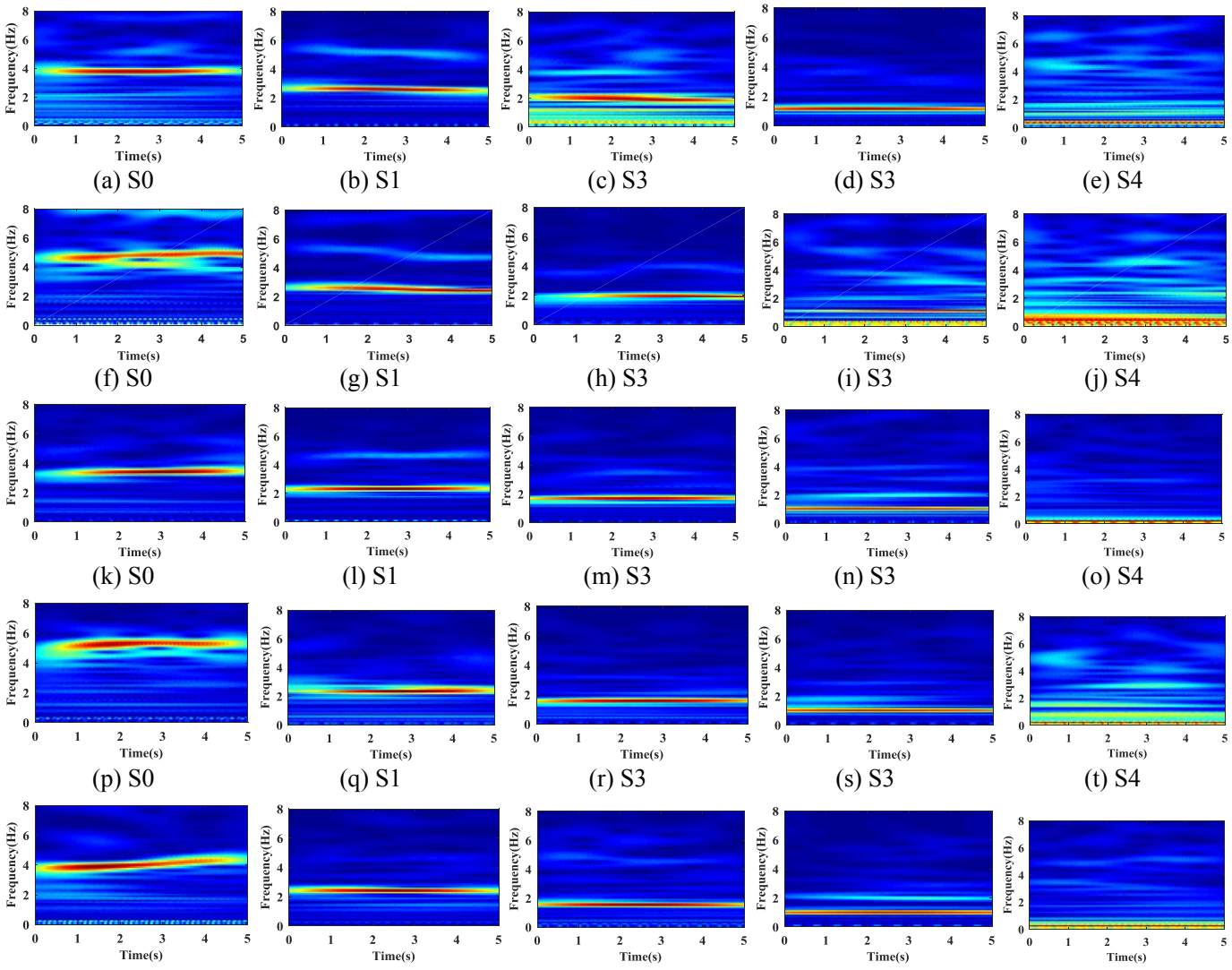


(a) S0 (b) S1 (c) S3 (d) S3 (e) S4

(f) S0 (g) S1 (h) S3 (i) S3 (j) S4

(k) S0 (l) S1 (m) S3 (n) S3 (o) S4

(p) S0 (q) S1 (r) S3 (s) S3 (t) S4

(u) S0 (v) S1 (w) S3 (x) S3 (y) S4

Fig. 7. Spectrum of finger tapping for all participants

The parameters of the kernel function and the penalty coefficient have a great influence on the performance of the SVM. In this paper, the more commonly used grid search method is used to find the SVM parameter method. It divides the parameters to be searched into a grid in a certain spatial range, and finds the optimal parameters by traversing all the points in the grid. We use scikit learn Python package to divide training set and test set, and then train SVM classifier. The accuracy of finger tapping with and without absorbent material was compared. The results are shown in Table III. Compared with the case without absorbing materials, the average quantization accuracy of phase difference and amplitude on finger tapping is improved by 2% and 1.2% respectively in the case of surrounded by absorbing materials. In addition, the quantification accuracy of the phase difference for finger tapping is better than the amplitude in these two scenarios.

TABLE III
COMPARISON OF QUANTIZATION ACCURACY OF PHASE DIFFERENCE AND AMPLITUDE FOR FINGER TAPPING

| | Data | S0 | S1 | S2 | S3 | S4 |
|---|---|---|---|---|---|---|
| With absorbing material | Phase difference | 1 | 1 | 0.98 | 0.98 | 0.99 |
| | Amplitude | 0.97 | 0.97 | 0.94 | 0.97 | 0.95 |
| Without absorbing material | Phase difference | 0.98 | 0.97 | 0.95 | 0.98 | 0.97 |
| | Amplitude | 0.96 | 0.95 | 0.93 | 0.95 | 0.95 |

In this study, five healthy volunteers participated in the experiment. After strict training, the volunteers imitated the patients with different severity of dyskinesia to perform finger tapping test. Table IV shows the quantification accuracy of finger tapping by five participants in simulating patients with different severity. We find that the quantization accuracy of the proposed system was more than 97% among different subjects. Even if the subjects are different, the proposed system shows good robustness.

TABLE IV
THE QUANTITATIVE ACCURACY OF THE PROPOSED SYSTEM FOR FINGER TAPPING OF DIFFERENT PARTICIPANTS

| | S0 | S1 | S2 | S3 | S4 |
|---|---|---|---|---|---|
| Participant 1 | 1 | 1 | 0.98 | 0.98 | 1 |
| Participant 2 | 1 | 1 | 0.99 | 0.97 | 0.99 |
| Participant 3 | 1 | 1 | 0.98 | 0.97 | 0.98 |
| Participant 4 | 1 | 1 | 0.97 | 0.99 | 1 |
| Participant 5 | 1 | 1 | 0.98 | 0.99 | 0.99 |

In addition, we compare the phase difference signal of the WCI with the gyroscope. The comparison results are shown in Fig. 9. The average recognition accuracy of the phase difference is 99.4%, and the average accuracy of the gyroscope to the five types is 97.3%. The phase difference signal and the gyroscope achieve 100% recognition accuracy when quantifying the three degrees of finger taps of 0, 1, and 4. However, the phase difference signal is superior to the gyroscope when the finger taps of the 2, 3 level is quantized. Therefore, our proposed wireless signal-based finger tap quantization system can achieve the same high-precision quantization level as wearable devices.

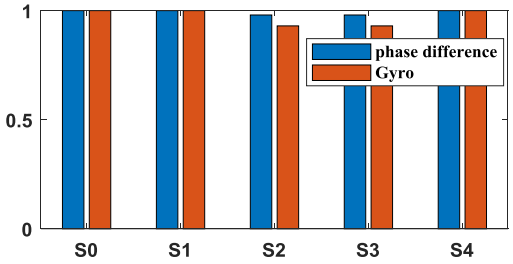

Fig. 9. Comparison of phase difference with gyro sensor.

Besides using SVM, we also try the other machine learning algorithms such as K- NN, RF. Figure 10 shows the overall accuracy of quantizing finger tapping based on multiple classifiers. We find that the accuracy of all classifiers is more than 90%, which verifies the robustness of the above processing methods and feature extraction. In addition, the accuracy of the quantized finger tapping model trained by SVM (Gaussian kernel function) is better than other classifiers.

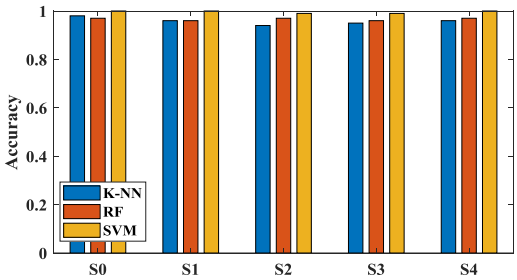

Fig. 10. Quantitative accuracy of finger tapping by different machine learning algorithms

## VI. CONCLUSION

This paper proposes novel, non-contact, a robust finger taps severity quantization system based on wireless signals to support autonomous hospital network. The cheap and efficient non-contact movement disorder quantification system can be used together with clinical test scores to provide diagnostic support and follow-up treatment. As with all motion detection systems based on wireless sensing technology, phase drift is a serious problem. To solve this problem, we calibrate the original phase by the phase difference between adjacent antennas. According to UPDRS, we extracted relevant time-domain features and used machine learning algorithms to achieve objective quantification of the finger tapping.

In the future, we hope to be able to verify and improve the proposed system in patients with dyskinesia, and assist clinicians in evaluating patients' motor function.

## REFERENCES

[1] Jankovic, J. "Parkinson's disease: clinical features and diagnosis," *J Neurol Neurosurg Psychiatry*, vol.79, pp.368-376, 2008.

[2] J. J. Hilten, Van, A. D. Zwan, Van Der, A. H. Zwinderman, and R. A. Roos, "Rating impairment and disability in Parkinson's disease: Evaluation of the unified Parkinson's disease rating scale," *Movement Disorders*, vol.9, pp.84-88, 1994.

[3] P. Pierleoni, A. Belli, O. Bazgir, L. Maurizi, M. Paniccia and L. Palma, "A Smart Inertial System for 24h Monitoring and Classification of Tremor and Freezing of Gait in Parkinson's Disease," *IEEE Sensors Journa*l, vol. 19, no. 23, pp. 11612-11623, 1 Dec.1, 2019.

[4] A. Kita, P. Lorenzi, R. Rao and F. Irrera, "Reliable and Robust Detection of Freezing of Gait Episodes With Wearable Electronic Devices," *IEEE Sensors Journal*, vol. 17, no. 6, pp. 1899-1908, 15 March15, 2017.

[5] Ventre-Dominey, J., Dominey, P.F., Broussolle, E. Dissociable processing of temporal structure in repetitive eye-hand movements in Parkinson's disease. Neuropsychologia,vol 40, pp.1407– 1418,2002.

[6] Shimoyama I, Ninchoji T, Uemura K. "The finger-tapping test: a quantitative analysis," *Archives of Neurology*, vol47, no.6, pp.681–4 ,1990.

[7] H. Dai, H. Lin, and T. C. Lueth, "Quantitative assessment of parkinsonian bradykinesia based on an inertial measurement unit," *Biomedical engineering online*, vol. 14, no. 1, p. 68, 2015.

[8] R. Claudia, M. Johan, S. Anne Margarethe, and V. H. J. M. D. Bob Johannes, "Systematic evaluation of rating scales for impairment and disability in Parkinson's disease," *Movement Disorders*, vol.17, no.5, pp.867–76,2002.

[9] O. Martinezmanzanera et al., "A method for automatic and objective scoring of bradykinesia using orientation sensors and classification algorithms". *IEEE Trans Biomed Eng*, vol.63, no.5, pp.1016-1024.2016.

[10] A. Salarian, H. Russmann, C. Wider, P. R. Burkhard, F. J. Vingerhoets, and K. Aminian, "Quantification of tremor and bradykinesia in Parkinson's disease using a novel ambulatory monitoring system," *IEEE Transactions on Biomedical Engineering*, vol. 54, no. 2, pp. 313-322, 2007.

[11] J.-W. Kim *et al.*, "Quantification of bradykinesia during clinical finger taps using a gyrosensor in patients with Parkinson's disease," *Med. Biol. Eng. Comput.*, vol. 49, no. 3, pp. 365–371, Mar. 2011.

[12] Milica D J, Nenad J, Agnes R B, et al.," Quantification of Finger-Tapping Angle Based on Wearable Sensors," *Sensors*, vol.17, no.2, pp.203,2017.

[13] R. Agostino, A. Currà, M. Giovannelli, N. Modugno, M. Manfredi, and A. Berardelli, "Impairment of individual finger movements in Parkinson's disease," Movement disorders, vol. 18, no. 5, pp. 560-565, 2003.

[14] Á. Jobbágy, P. Harcos, R. Karoly, and G. Fazekas, "Analysis of finger-tapping movement," Journal of neuroscience methods, vol. 141, no. 1, pp. 29-39, 2005.

[15] H. Dai, G. Cai, Z. Lin, Z. Wang, and Q. Ye, "Validation of Inertial Sensing-based Wearable Device for Tremor and Bradykinesia Quantification," *IEEE Journal of Biomedical and Health Informatics*, 2020.

[16] E. L. Stegemöller, T. Simuni, and C. MacKinnon, "Effect of movement frequency on repetitive finger movements in patients with Parkinson's disease," *Movement Disorders*, vol. 24, no. 8, pp. 1162-1169, 2009.

[17] M. Yokoe, R. Okuno, T. Hamasaki, Y. Kurachi, K. Akazawa, and S. Sakoda, "Opening velocity, a novel parameter, for finger tapping test in patients with Parkinson's disease," *Parkinsonism and Related Disorders*, vol. 15, no. 6, pp. 440–444, 2009.

[18] E. L. Stegemöller, T. Simuni, and C. MacKinnon, "Effect of movement frequency on repetitive finger movements in patients with Parkinson's disease," *Movement Disorders*, vol. 24, no. 8, pp. 1162-1169, 2009.

[19] S. Julien et al., "Finger tapping clinimetric score prediction in Parkinson's disease using low-cost accelerometers," *Computational Intelligence and Neuroscience*, vol.2013, no. 2, pp. 1, 2013.

[20] Y. Sano et al., "Quantifying Parkinson's disease finger-tapping severity by extracting and synthesizing finger motion properties," *Medical & Biological Engineering & Computing*, vol. 54, no. 6, pp.1-13,2016.

[21] T. Khan, D. Nyholm, J. Westin, and M. J. A. I. i. M. Dougherty, "A computer vision framework for finger-tapping evaluation in Parkinson's disease," Artificial Intelligence in Medicine, vol. 60, no. 1, pp. 27-40, 2014.

[22] S. Williams *et al.*, "The discerning eye of computer vision: Can it measure Parkinson's finger tap bradykinesia?" *Journal of the Neurological Sciences*, vol. 416, p. 117003, 2020.

[23] Y. Pang et al., "Automatic detection and quantification of hand movements toward development of an objective assessment of tremor and bradykinesia in Parkinson's disease," *Journal of Neuroscience Methods*, vol. 333, p. 108576, 2020.

[24] Z. Zhou, Z. Yang, C. Wu, L. Shangguan, and Y. Liu, "Towards omnidirectional passive human detection," in *Proc. IEEE INFOCOM*, Apr. 2013, pp. 3057–3065

[25] S. Sen, J. Lee, K.-H. Kim, and P. Congdon, "Avoiding multipath to revive inbuilding WiFi localization," in *Proc. ACM MobiSys*, 2013, pp. 249–262.

[26] R. Zhou, X. Lu, P. Zhao and J. Chen, "Device-Free Presence Detection and Localization With SVM and CSI Fingerprinting," in IEEE Sensors Journal, vol. 17, no. 23, pp. 7990-7999, 1 Dec.1, 2017, doi: 10.1109/JSEN.2017.2762428.

[27] W. Xi *et al.*, "Electronic frog eye: Counting crowd using WiFi," in *Proc. IEEE INFOCOM*, May 2014, pp. 361–369.

[28] O. T. Ibrahim, W. Gomaa, and M. Youssef, "CrossCount: A Deep Learning System for Device-Free Human Counting Using WiFi," *IEEE Sensors Journal*, vol. 19, no. 21, pp. 9921-9928, 2019.

[29] Y. Wang, J. Liu, Y. Chen, M. Gruteser, J. Yang, and H. Liu, "E-eyes: Device-free location-oriented activity identification using fine-grained WiFi signatures," in *Proc. ACM MobiCom*, 2014, pp. 617–628.

[30] W. Wang, A. X. Liu, M. Shahzad, K. Ling and S. Lu, "Device-Free Human Activity Recognition Using Commercial WiFi Devices," I*EEE Journal on Selected Areas in Communications*, vol. 35, no. 5, pp. 1118-1131

[31] Q. Pu, S. Gupta, S. Gollakota, and S. Patel, ''Whole-home gesture recognition using wireless signals,'' in *Proc. 19th Annu. Int. Conf. Mobile Comput.Netw.*, 2013, pp. 27–38.

[32] H. Yan, Y. Zhang, Y. Wang and K. Xu, "WiAct: A Passive WiFi-Based Human Activity Recognition System," *IEEE Sensors Journal*, vol. 20, no. 1, pp. 296-305, 1 Jan.1, 2020.

[33] F. Dou, A. Ren, Z. Nan, X. Yang, Z. Zhang, S. A. Shah, F. Hu, and Q. H. J. I. A. Abbasi, "Breathing Rhythm Analysis in Body Centric Networks," *IEEE Access*, vol. 6, pp. 1-1, 2018.

[34] G. Wang, Y. Zou, Z. Zhou, K. Wu, and L. M. Ni, "We can hear you with Wi-Fi!" in *Proc. ACM MobiCom*, Nov. 2014, pp. 2907–2920.

[35] K. Ali, A. X. Liu, W. Wang, and M. Shahzad, "Keystroke recognition using WiFi signals," in *Proc. ACM MobiCom*, 2015, pp. 90–102.

[36] L. Zhang and H. Wang, "Device-Free Tracking via Joint Velocity and AOA Estimation With Commodity WiFi," *IEEE Sensors Journal*, vol. 19, no. 22, pp. 10662-10673, 2019.

[37] X. Wang, C. Yang, and S. Mao, "Resilient Respiration Rate Monitoring with Realtime Bimodal CSI Data," *IEEE Sensors Journal*, 2020.

[38] J. Gjengset, J. Xiong, G. McPhillips, and K. Jamieson, ''Phaser: Enabling phased array signal processing on commodity WiFi access points,'' in *Proc. Int. Conf. Mobile Compute. Network.*, 2014, pp. 153–164.

[39] H. C. Liu, S. Shah, W. J. C. Jiang, and C. Engineering, "On-line outlier detection and data cleaning," *Computers& Chemical Engineering*,vol. 28, no. 9, pp. 1635-1647, 2004.

[40] O. Rioul et al., "Fast Algorithm for Discrete and Continuous Wavelet Transforms," *IEEE Trans Inform Theory*, vol. 38, no. 2, pp. 569-586, 1992.